MOLECULAR AND CELLULAR BIOLOGY, Dec. 1997, p. 7375–7385 Vol. 17, No. 12
0270-7306/97/$04.00+0
Copyright © 1997, American Society for Microbiology

IκBα Physically Interacts with a Cytoskeleton-Associated Protein through Its Signal Response Domain

PASCALE CRÉPIEUX,[1,2] HAKJU KWON,[1,2] NICOLE LECLERC,[3] WILLIAM SPENCER,[1,4] STÉPHANE RICHARD,[1,2] RONGTUAN LIN,[1,2] AND JOHN HISCOTT[1,2,4]*

Terry Fox Molecular Oncology Group, Lady Davis Institute for Medical Research,[1] and Departments of Microbiology[4] and Medicine,[2] McGill University, Montreal, Canada H3T 1E2, and Department of Pathology,[3] University of Montreal, Montreal, Canada H3C 3J7

Received 11 December 1996/Returned for modification 14 February 1997/Accepted 26 August 1997

The IκBα protein is a key molecular target involved in the control of NF-κB/Rel transcription factors during viral infection or inflammatory reactions. This NF-κB-inhibitory factor is regulated by posttranslational phosphorylation and ubiquitination of its amino-terminal signal response domain that targets IκBα for rapid proteolysis by the 26S proteasome. In an attempt to identify regulators of the IκBα inhibitory activity, we undertook a yeast two-hybrid genetic screen, using the amino-terminal end of IκBα as bait, and identified 12 independent interacting clones. Sequence analysis identified some of these cDNA clones as Dlc-1, a sequence encoding a small, 9-kDa human homolog of the outer-arm dynein light-chain protein. In the two-hybrid assay, Dlc-1 also interacted with full-length IκBα protein but not with N-terminal-deletion-containing versions of IκBα. IκBα interacted in vitro with a glutathione *S*-transferase–Dlc-1 fusion protein, and RelA(p65) did not displace this association, demonstrating that p65 and Dlc-1 contact different protein motifs of IκBα. Importantly, in HeLa and 293 cells, endogenous and transfected IκBα coimmunoprecipitated with Myc-tagged or endogenous Dlc-1. Indirect immunofluorescence analyzed by confocal microscopy indicated that Dlc-1 and IκBα colocalized with both nuclear and cytoplasmic distribution. Furthermore, Dlc-1 and IκBα were found to associate with the microtubule organizing center, a perinuclear region from which microtubules radiate. Likewise, IκBα colocalized with α-tubulin filaments. Taken together, these results highlight an intriguing interaction between the IκBα protein and the human homolog of a member of the dynein family of motor proteins and provide a potential link between cytoskeleton dynamics and gene regulation.

The cytoskeleton can be considered a complex biological network that integrates signal transduction pathways and responds by altering the pattern of gene expression and by changing cell morphology. Reorganization of structural components within the cytoskeleton can achieve these changes by exposing or masking internal molecular binding sites (32). For example, changes in the arrangement of cytoskeletal filaments may expose sequestered RNA molecules to cytoplasmic enzymes to which they were otherwise resistant (50). Recently, the Rho family of G proteins has become a paradigm of the link between actin cytoskeleton modifications and gene expression in response to growth factors (for a review, see reference 18). For example, phosphatidylinositol 3-kinase-mediated activation of Rac proteins by platelet-derived growth factor or insulin receptors (52) leads to membrane ruffling on the one hand and stimulation of the p21-associated kinases that control JNK/SAPK (18) and the mitogen-activated protein kinases (MAPKs) (25) on the other hand, leading to gene expression.

The microtubule cytoskeleton also is involved in modulation of gene expression. Microtubule-disrupting agents such as colchicine have been reported to induce interleukin-1 expression in monocytes (45) or AP1-regulated urokinase-type plasminogen activator transcription (41). To date, the molecular events that link microtubule disruption to signal transduction pathways are poorly characterized. However, during monocyte differentiation, tubulin becomes phosphorylated, and Fyn and Lyn have been proposed as candidate protein tyrosine kinases involved in this process (35). In addition, MAPKs have been shown to associate with and destabilize microtubules by phosphorylation of microtubule-associated proteins, hence their original name (55).

The activity of some cytoplasmic transcription factors which migrate to the nucleus upon stimulation can be modulated by cytoskeletal plasticity. This is the case with the NF-κB/Rel family of transcription factors, which preexist as a latent complex in the cytoplasm of unstimulated cells (6). Cytosolic retention is mediated by the IκB family of inhibitory proteins (7, 10, 27). The IκB inhibitory molecules are all characterized by the presence of five to seven ankyrin motifs, responsible for p65 association and DNA-binding inhibition (29, 33, 34), and are also thought to mediate cytoskeleton association through these motifs (44). To date, the most extensively characterized IκB family member has been the IκBα protein. Upon cell stimulation, IκBα is inducibly degraded, thus unmasking the nuclear localization signal of the NF-κB subunits and permitting nuclear translocation and gene activation (70). The molecular events that lead to rapid IκBα proteolysis converge upon a signal response domain located at the amino-terminal end of the inhibitor (12, 13). Phosphorylation of ^{32}Ser and ^{36}Ser (13, 15, 66) targets IκBα for ubiquitination on ^{21}Lys and ^{22}Lys (57, 59) and subsequent proteolytic degradation by the 26S proteasome multisubunit complex (3, 15, 65). Despite considerable discrepancies between in vivo and in vitro data, it appears that these posttranslational modifications occur while IκBα is still bound to the NF-κB subunits (2, 20, 23, 43, 46). The carboxy-terminal portion of IκBα contains an acid-rich region, the PEST region, which has been reported to be responsible for constitutive turnover of IκBα (9, 42).

Since the IκBα protein is a key molecular target specifically

* Corresponding author. Mailing address: Lady Davis Institute for Medical Research, 3755 Cote Ste. Catherine, Montreal, Que. H3T 1E2, Canada. Phone: 514-340-8222, ext. 5265. Fax: 514-340-7576. E-mail: mijh@musica.mcgill.ca.

controlling NF-κB activity during viral infection or inflammatory reactions, it is of crucial interest to precisely characterize the effectors, i.e., the kinase(s) and protease(s) that mediate inducible IκBα degradation. A 700-kDa multisubunit complex that requires ubiquitination for activity has been isolated as a potential IκBα kinase activity (16); recent experiments also implicate MEKK1 in the signaling cascade leading to IκBα kinase activation (40). Interestingly, a novel proteolysis-independent mechanism of NF-κB activation, mediated through ^{42}Tyr phosphorylation of IκBα, has also been reported (31).

In order to identify regulators of the IκBα inhibitory activity, we undertook a yeast two-hybrid genetic screen, using the regulatory amino-terminal end of IκBα as bait. In this report, we provide evidence for a novel interaction between IκBα and Dlc-1, a cytoskeleton-associated protein.

MATERIALS AND METHODS

Cell culture. COS-1, HeLa and N-Tera 2 cells were grown in minimal essential medium containing 10% fetal bovine serum. Myeloid cell lines (ZR3, U937, PLB-985, and H460), the T-cell lines Jurkat and Jurkat-IIIB (a human immunodeficiency virus type 1-infected Jurkat line) and the B-lymphoblastoid cell line Raji were grown in suspension in RPMI 1640 containing 10% fetal bovine serum. Media were supplemented with gentamicin (10 μg/ml) as previously described (61).

Yeast two-hybrid screen. The fragment containing the amino-terminal 55 amino acids (aa) of IκBα (NIK) and the NIK2N fragment were PCR amplified with primer A (5′-GATCGTCGACAGCTCGTCCGCGCCATGTTC-3′) and B (5′-GTCCGTCGACCTCGGTGAGCTGCTGCTTCC-3′) and subcloned into the *Sal*I site of the *TRP1* pBTM116 vector, in frame with the LexA DNA-binding domain. After transformation of the L40 yeast strain [*MAT*α *his3*Δ*200 trp1-901 leu2-3 ade2 LYS2*::(*lexAop*)$_4$-*HIS3 URA3*::(*lexAop*)$_8$-*LACZ GAL4*] (30) by the lithium acetate permeabilization method (60) and selection for tryptophan prototrophy, the NIK-expressing clone was cotransformed with an LMP-1-transformed B-cell cDNA library cloned into the *LEU2* pACT2 vector (Clontech), according to the Matchmaker protocol. Positive yeast clones were selected for prototrophy for histidine and expression of β-galactosidase. Subsequent two-hybrid assays were carried out by a mating assay between the AMR70 *MAT*α tester strain [*MAT*α *his3 lys2 trp1 leu2 URA3*::(*lexAop*)$_8$-*LACZ GAL4*] (30) and the L40 strain. Diploid cells from the mating assay were selected on Trp$^-$ Leu$^-$ His$^-$ selective medium and screened by replica plating for their ability to produce β-galactosidase. The full-length IκBα gene and those for the carboxy-terminal PEST-containing domain of IκBα (CIK) and ankyrin repeat region (ANK) constructs were all subcloned into the pGAD424 vector (Clontech), in frame with the *GAL4* transactivation domain. The IκBα gene was PCR amplified from a pSVK3 construct (8) with primer A described above and primer C (5′-CCCCTGCAGGTCGACTCTAGAG-3′), homologous to the pSVK3 vector polylinker, and subcloned into the *Sal*I site; the CIK fragment sequence was inserted into the *Sma*I and *Sal*I sites, and the ANK fragment sequence was subcloned into the *Eco*RI and *Sma*I sites. The pBTM116 derivatives and the laminin- and ras-expressing plasmids were gifts from S. Katzav (Hebrew University, Jerusalem, Israel), and the NFATc construct was a gift from L. Petropoulos. These controls were all subcloned into pBTM116 derivatives. The subsequent subclonings were performed after PCR amplification of the Dlc-1 insert in pACT2, with pACT2-specific primers, as described in the Matchmaker protocol.

GST-affinity chromatography. Bacterially synthesized IκBα and IκBα2N (100 ng) were incubated with glutathione *S*-transferase (GST) or GST–Dlc-1 (1 μg) for 1.5 h at room temperature in phosphate-buffered saline (PBS)–0.1% Triton. After four washes in PBS–0.1% Triton, complexes were analyzed by Western blotting. Purified IκBα (2 ng) was loaded as a migration control. Immunodetection was performed with the rabbit anti-IκBα polyclonal antibody. The same procedure was used to visualize p65-IκBα-Dlc-1 interaction, except that the amounts of the different proteins varied (as described in Results).

Immunoprecipitation. The Dlc-1 partial cDNA was subcloned into the pBluescript KS plasmid, in frame with a Myc epitope tag, as previously described (56). After infection with vaccinia virus to sustain high levels of T7 RNA polymerase-dependent transcription, HeLa cells were transfected with Myc-tagged Dlc-1-expressing plasmid and harvested after 6 h of incubation at 37°C (26). Cells were then lysed in PBS–0.5% Nonidet P-40. Total cell lysates (100 μg) were immunoprecipitated with a monoclonal anti-IκBα antibody (MAD10B) for 1.5 h at 4°C, and immune complexes were then used to coat protein A-Sepharose for an additional 0.5 h at 4°C. After four washes in PBS–0.5% Nonidet P-40, complexes were analyzed by Western blotting. Crude extracts (10 μg) were loaded as migration controls. Immunodetection was performed with an anti-Myc monoclonal antibody. In some experiments, 293 cells were transfected with SVK3-IκBα and Myc-tagged Dlc-1 (10 μg each) by the calcium phosphate method, and at 48 h after transfection, cells were treated for 15 or 30 min with 10 ng of tumor necrosis factor alpha (TNF-α) (R&D Systems) per ml to degrade IκBα. Lysates were prepared as described above. Total cell lysates (300 μg) were immunoprecipitated with a C-terminal anti-IκBα antibody (Santa Cruz, Inc.) for 1.5 h at 4°C; immune complexes were isolated on protein A-Sepharose for an additional hour at 4°C, and the immunoprecipitates were analyzed with an anti-Myc monoclonal antibody. Anti-GST–Dlc-1 antibody was also used to immunoprecipitate Dlc-1 complexes from 293 cell lysates (1 to 3 mg); immune complexes were then isolated on protein A-Sepharose for an additional hour at 4°C. After four washes in PBS–0.5% Nonidet P-40, immunoprecipitates were analyzed for IκBα by Western blotting with anti-N-terminal IκBα (Santa Cruz). Crude extracts (20 μg) were loaded as migration controls.

Preparation of cytoplasmic and nuclear extracts. Jurkat and N-Tera 2 cells seeded at 10^6/ml were treated with 10 ng of TNF-α per ml of culture medium for 15 min at 37°C, washed twice in PBS, and then collected after each washing by centrifugation. Sedimented cells were gently resuspended and disrupted for 10 min in lysis buffer containing 10 mM HEPES (pH 7.9), 1.5 mM $MgCl_2$, 10 mM KCl, 0.5 mM dithiothreitol (DTT), 0.5 mM phenylmethylsulfonyl fluoride (PMSF), and 0.1% Nonidet P-40. After 40 μl of supernatant was collected to prepare the cytoplasmic extracts, sedimented nuclei were further disrupted for 15 min in 20 mM HEPES (pH 7.9), 1.5 mM $MgCl_2$, 0.5 mM DTT, 0.5 mM PMSF, 25% glycerol, 0.42 M NaCl, and 0.2 mM EDTA in the presence of 5 μg of each of the following protease inhibitors per ml: leupeptin, pepstatin, spermidine, spermine, and aprotinin. After centrifugation, nuclear extracts were collected and stored as a fivefold dilution in 20 mM HEPES (pH 7.9), 0.5 mM DTT, 0.5 mM PMSF, 20% glycerol, 0.2 mM EDTA, and 50 mM KCl.

Transfection of DNA plasmids in mammalian cells. HeLa cells were transfected with 5 μg of Myc-tagged Dlc-1 as previously described (56), except that Lipofectamine (GIBCO) was used. COS-1 cells were transfected on plastic eight-well slides, with 125 ng of DNA per well, with Lipofectamine. The transfected DNAs were those corresponding to NF-κB RelA(p65) and Myc-tagged Dlc-1, both subcloned into the pSVK3 expression plasmid.

Western blot analysis and antibodies. Unless otherwise indicated, 40 μg of proteins from each sample was fractionated in a sodium dodecyl sulfate-polyacrylamide gel (10% acrylamide for the detection of IκBα and 15% acrylamide for the detection of Dlc-1 and α tubulin), electrophoretically transferred to a Hybond C nitrocellulose membrane (Amersham), and probed with various antibodies, as follows. To detect IκBα, a murine monoclonal IκBα antibody raised against human IκBα aa 21 to 48 (a generous gift from R. T. Hay, University of St. Andrews, Fife, Scotland) or rabbit polyclonal anti-IκBα antibody previously described (53) was used. In some experiments N- and C-terminus-specific antibodies were used (Santa Cruz). p65NF-κB was detected with a rabbit polyclonal antiserum directed against residues 29 to 45 of human p65 (53). Recombinant Dlc-1 cDNA was used to generate a GST–Dlc-1 fusion construct, and the GST fusion protein was used to raise a rabbit polyclonal antibody. The antisera were precleared on GST beads before use. The anti-Myc monoclonal antibody 9E10 was raised against aa 410 to 419 of human c-Myc (22). The monoclonal anti-human α-tubulin antibody was purchased from Sigma. Horseradish peroxidase-coupled anti-rabbit and anti-mouse antibodies were used to detect specific antigen-antibody interactions by enhanced chemiluminescence (ECL kit; Amersham).

Indirect immunofluorescence and confocal microscopy. Cells were fixed in plastic eight-well chambers in paraformaldehyde (3% in PBS), and indirect immunofluorescence was performed as previously described (53). Unless otherwise stated, rhodamine-coupled secondary anti-mouse antibody was used to detect Myc-tagged Dlc-1, and a fluorescein-coupled anti-rabbit secondary antibody allowed detection of IκBα. Both secondary antibodies were purchased from Jackson Laboratories. Slides were analyzed on a Leitz fluorescence microscope (Aristoplan). A laser scanning Bio-Rad MRC600 microscope was used for confocal microscopy analysis.

Nucleotide sequence accession numbers. The Dlc-1 sequences have been deposited in GenBank as follows: *Chlamydomonas reinhardtii*, U19490; *Schistosoma mansoni*, U55992; *Caenorhabditis elegans*, U00043; *Drosophila melanogaster*, U32855; and *Homo sapiens*, U32944.

RESULTS

Isolation of Dlc-1 as an IκBα-interacting protein in yeast. In an attempt to identify novel IκBα-interacting partners, an LMP-1-transformed B-cell cDNA library was screened with NIK as bait. From 3×10^6 cotransformants, 4,000 clones prototrophic for histidine were selected, among which 750 were also able to activate the β-galactosidase reporter gene (Fig. 1). The specificity of 250 clones was assessed by mating the segregated L40 strain to the AMR70 strain, expressing NIK, full-length IκBα, or unrelated proteins such as ras, laminin, and NFATc. From this extensive screening, we isolated 12 clones specifically interacting with NIK. Their inserts were PCR amplified with the pACT2-specific primers, and Southern blot

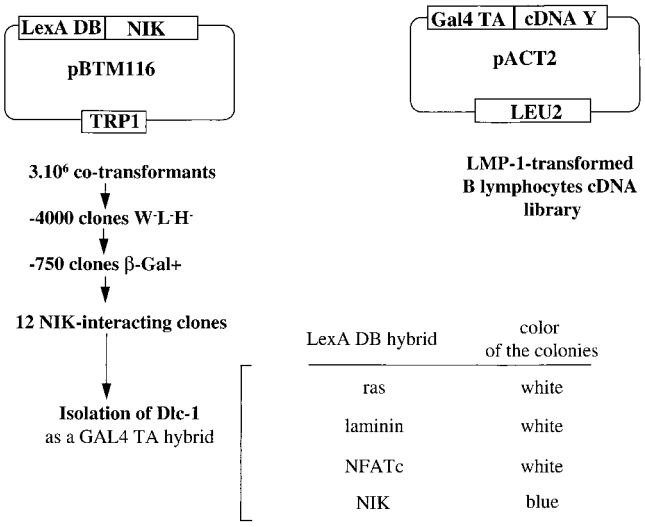

FIG. 1. Two-hybrid screen of the human LMP-1-transformed B-lymphocyte cDNA library with the amino-terminal end of IκBα (NIK, aa 1 to 55) as a LexA DNA-binding domain fusion protein. The L40 yeast strain was transformed with NIK subcloned into the pBTM116 vector. The resulting strain was cotransformed with the cDNA library in pACT2. To control NIK–Dlc-1 interaction specificity, yeast expressing only Dlc-1 was segregated and then mated to the AMR70 strain expressing laminin, ras, or NFATc in fusion with the LexA DNA-binding domain. Control yeast cotransformations with Dlc-1 and empty LexA and Gal4 vectors were negative and are not listed here.

analysis indicated that eight of the clones were homologous (data not shown). Sequencing and database analysis identified two of these eight as Dlc-1, a human homolog of the *C. reinhardtii* 8-kDa outer-arm dynein light chain (Fig. 2) (37). In a two-hybrid assay, the corresponding clone specifically interacted with NIK and not with ras, laminin, or NFATc (Fig. 1). The PCR-amplified Dlc-1 DNA fragment was 503 bp long and contained the entire coding sequence except that for the two amino-terminal amino acids of the 9-kDa protein (data not shown). One of the encoded proteins (Dlc-1b) differed at the carboxy-terminal end from the sequence reported previously (19). This difference is likely due to alternative splicing since both cDNA sequences are colinear at the 5′ and 3′ ends, except for the carboxy-terminal coding regions of Dlc-1a and Dlc-1b. In addition, a sequence similar to Dlc-1b is present in the GenBank database, thus ruling out the possibility of a chimeric cDNA in the library. In subsequent experiments, we refer to the clones as Dlc-1 to designate both isoforms, since they are indistinguishable. Comparison of the various Dlc-1 polypeptide sequences from different sources revealed a strikingly high degree of conservation between distant species, pointing to the conservation of a crucial cellular function(s) (Fig. 2).

The amino-terminal end of IκBα is sufficient for association with Dlc-1. To investigate whether Dlc-1 interacted specifically with NIK or with other domains of IκBα, a two-hybrid analysis was performed with various deletion-containing versions of IκBα. Since full-length IκBα, as well as ANK and CIK constructs, transactivated the His3 and β-galactosidase reporter genes (18a, 47, 48), the proteins were expressed as Gal4 transactivation domain hybrids from the pGAD424 vector. The other constructs were expressed as LexA DNA-binding fusions from the pBTM116 vector. Dlc-1 interacted with NIK and with full-length IκBα (Fig. 3) but not with deletion versions containing ANK or CIK, indicating that only the N-terminal signal response domain of IκBα (aa 1 to 55) was required for interaction. Interestingly, Dlc-1 also interacted efficiently with NIK2N, a construct in which ^{32}Ser and ^{36}Ser were mutated to Ala.

To confirm the specific interaction of Dlc-1 with IκBα observed in the two-hybrid assay, we next performed in vitro GST affinity chromatography (Fig. 4). A GST fusion protein containing Dlc-1 was tested for interaction with full-length IκBα (Fig. 4A). Purified IκBα (Fig. 4A, lane 2), as well as IκBα2N (Fig. 4A, lane 3), was efficiently pulled down by GST–Dlc-1 but not by the GST moiety alone (Fig. 4A, lane 1). Conversely, GST-IκBα also interacted with purified Dlc-1 in vitro (see Fig. 5A). Having demonstrated in vitro association, we next examined whether Dlc-1 also associated with IκBα in vivo. An expression vector that directs the synthesis of Dlc-1 (aa 3 to 80) fused to an amino-terminal Myc epitope tag was transfected into HeLa cells. At 6 h after transfection, extracts were prepared and immunoprecipitated with an IκBα antibody (MAD10B); coimmunoprecipitated proteins were fractionated by sodium dodecyl sulfate-polyacrylamide gel electrophoresis and immunoblotted with anti-Dlc-1 antibody. IκBα antibody coimmunoprecipitated Dlc-1 that migrated at the same size as HeLa extracts overexpressing Myc-tagged Dlc-1 (Fig. 4B, lanes 2 and 3). As determined by this assay, endogenous IκBα interacted with Dlc-1 in HeLa cells transfected with the expression vector. In contrast, this band was not visible in untransfected HeLa cells (Fig. 4B, lane 1). The upper band in the Western blot represents the detection of mouse immunoglobulins. For 293 cells cotransfected with both SVK3-IκBα and Myc–Dlc-1, lysates were prepared and immunoprecipitated with C-terminal anti-IκBα antibody and analyzed for Dlc-1 in the coprecipitate with the anti-Myc monoclonal antibody. No Dlc-1 was precipitated when preimmune serum was used (Fig. 4C, lane 1); however, Dlc-1 was detected in the immunoprecipitate when anti-IκBα antibody was used (Fig. 4C, lane 2). Interestingly, TNF treatment which degrades IκBα and should disrupt IκBα-Dlc-1 interaction resulted in a loss of Dlc-1 in the IκBα precipitate after 30 min of TNF treatment (Fig. 4C, lanes 3 and 4). Finally, by using anti-GST–Dlc-1, an endogenous Dlc-1–IκBα complex was immunoprecipitated from 293 cell lysates; IκBα precipitated by anti-GST–Dlc-1 (Fig. 4D, lane 1) migrated in an immunoblot at the same position as endogenous IκBα which had been immunoprecipitated first with rab-

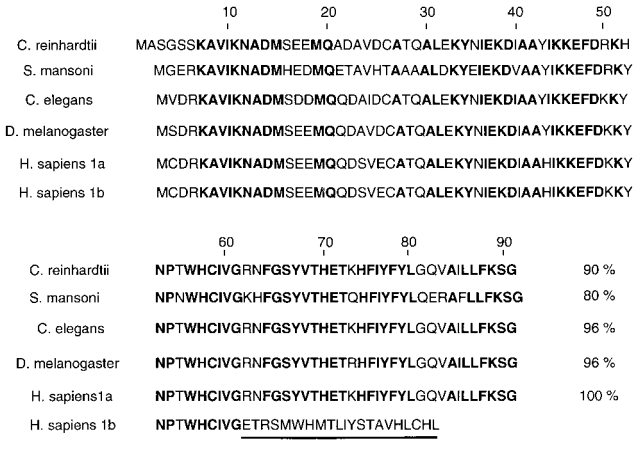

FIG. 2. Sequence alignment of Dlc-1 in different species. Identical amino acids are in bold letters. Homology to the human Dlc-1a protein is indicated. Dlc-1a refers to the Dlc-1 sequence reported elsewhere (19); Dlc-1b refers to the alternatively spliced form of Dlc-1, which has been previously identified and also detected in the present two-hybrid screen. Dlc-1b amino acids which differ from those in Dlc-1a are underlined.

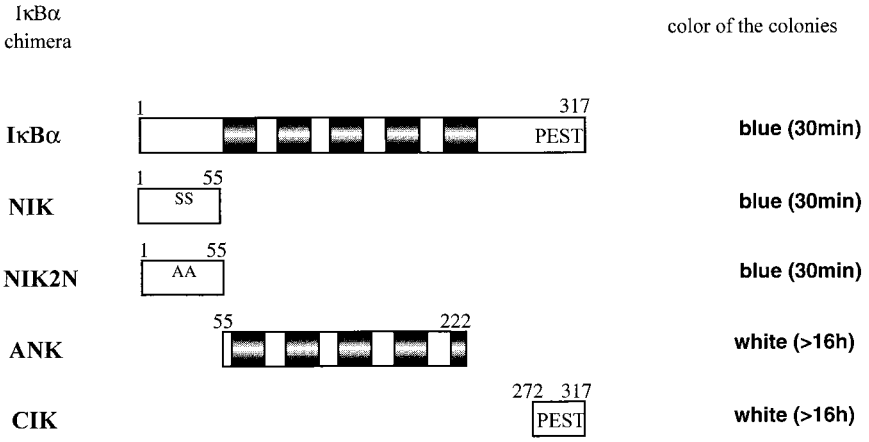

FIG. 3. Dlc-1 interacts with the signal response domain but not with other regions of IκBα. NIK, NIK2N, and full-length IκBα interacted with Dlc-1 but not the ANK and CIK constructs. Dlc-1-expressing L40 yeasts were mated to the AMR70 yeast strain expressing the different IκBα constructs as either LexA DNA-binding domain hybrids (NIK and NIK2N), or Gal4 transactivation domain hybrids (IκBα, ANK, and CIK). The color of the colonies reflects β-galactosidase activity as tested by replica plating. Blue colonies are indicative of a positive interaction (color formation within 30 min), and white colonies indicate a lack of interaction (>16 h).

bit anti-C-terminal IκBα antibody and then immunoblotted with anti-MAD10B (Fig. 4D, lane 2). Both these bands comigrated with endogenous IκBα present in the whole-cell lysate (Fig. 4D, lane 4). In conclusion, the interaction between IκBα and Dlc-1 demonstrated by the yeast two-hybrid assay and in vitro GST affinity analyses reflects the in vivo association of these two proteins.

Dlc-1 and p65 simultaneously bind different domains of IκBα in vitro. Next we investigated whether the interaction between IκBα and Dlc-1 could be prevented by RelA(p65) binding to IκBα, either by steric hindrance or by conformational change. For this purpose, GST–Dlc-1 was preincubated with 50 ng of IκBα and different amounts of Np65 (an amino-terminal polypeptide of RelA, aa 1 to 328). The addition of increasing amounts of Np65 did not significantly modify IκBα–Dlc-1 interaction (Fig. 5A). Conversely, preincubation of GST–IκBα with increasing amounts of Dlc-1 did not alter IκBα association with Np65 (Fig. 5B). In addition, this experiment also indicates that Dlc-1 does not interact directly with Np65 (Fig. 5A, lane 7). Therefore, Dlc-1 binds to IκBα through its amino-terminal end without compromising its capacity to interact with p65 through the ankyrin repeats.

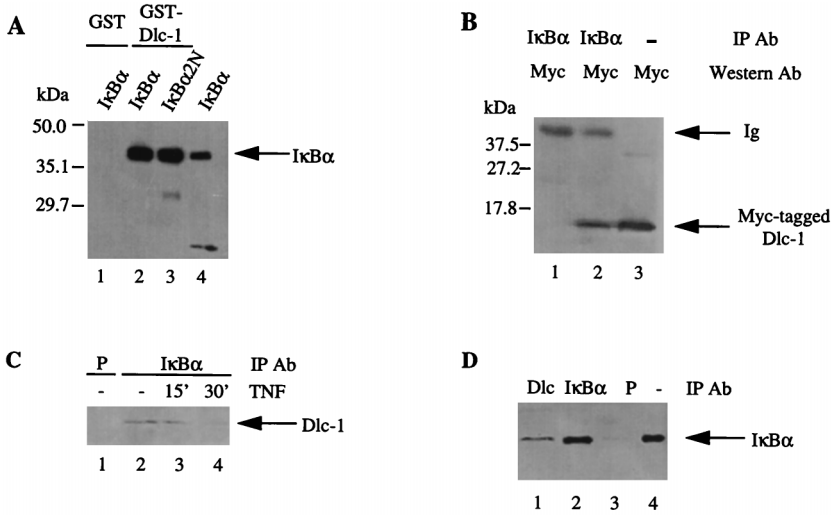

FIG. 4. Dlc-1 and IκBα interact in vitro and in vivo. (A) In vitro interaction of Dlc-1 and IκBα. GST (lane 1) and GST–Dlc-1 (lanes 2 and 3) were incubated with IκBα (lanes 1 and 2) or IκBα2N (lane 3). Lane 4 shows crude bacterial extract of IκBα protein as a migration control. Western blot analysis was performed with the anti-IκBα antibody (AR20). The lower bands in lanes 3 and 4 are degradation products of IκBα. (B) In vivo interaction of Dlc-1 and IκBα. Lysates of HeLa cells transfected (lanes 2 and 3) with Myc-tagged Dlc-1 or untransfected (lane 1) were immunoprecipitated with the anti-IκBα antibody (lanes 1 and 2). Lane 3 shows migration of crude transfected HeLa extracts as a control. Western blot analysis was performed using the anti-Myc antibody. (C) In vivo interaction of Dlc-1 and IκBα. 293 cells were transfected with SVK3-IκBα and Myc-tagged Dlc-1 (10 μg each); at 48 h after transfection, cells were treated for 15 or 30 min with 10 ng of TNF-α (R&D Systems) per ml to degrade IκBα, and lysates were prepared. Total cell lysates (300 μg) were immunoprecipitated with a C-terminal anti-IκBα antibody (Santa Cruz, Inc.), and the immunoprecipitates were analyzed for Dlc-1 by immunoblot with an anti-Myc antibody. The antibody used in the immunoprecipitation step is indicated above the lane; P, preimmune serum. (D) In vivo interaction of Dlc-1 and IκBα. Anti-GST–Dlc-1 antibody was also used to immunoprecipitate endogenous Dlc-1 complexes from 293 cell lysates (1 to 3 mg); immune complexes were then isolated on protein A-Sepharose and analyzed for IκBα by Western blot with anti-N-terminal IκBα (Santa Cruz, Inc.). Whole-cell extracts (20 μg) were loaded as migration controls. The antibody used in the immunoprecipitation step is indicated above the lane; P, preimmune serum.

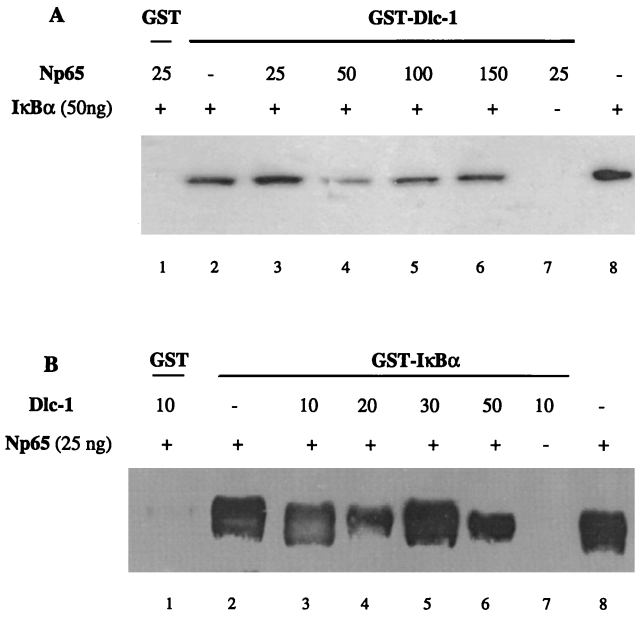

FIG. 5. Dlc-1 and NF-κB RelA contact different protein motifs on IκBα. (A) GST–Dlc-1 and IκBα association cannot be displaced by increasing amounts of Np65 (lanes 2 to 6). p65 and IκBα are not retained aspecifically by GST (lane 1), while p65 does not interact directly with GST-Dlc-1 (lane 7). Immunodetection was performed with the anti-IκBα antibody. Migration of purified IκBα is shown in lane 8. (B) GST-IκBα and Np65 interaction cannot be displaced by increasing amounts of Dlc-1 (lanes 2 to 6). p65 and Dlc-1 are barely retained by GST (lane 1). Western blot analysis allows detection of Np65. Lane 8 shows an Np65 migration control.

Ubiquitously expressed Dlc-1 displays nuclear and cytoplasmic localization. To further investigate the expression pattern of hDlc-1, protein and RNA samples from several different fibroblastic and hematopoietic cells were analyzed for hDlc-1 expression. Although the levels of expression varied from one cell type to another, all cells examined constitutively expressed hDlc-1 at both the RNA and protein levels (Fig. 6A and B). Dlc-1 distribution was also analyzed biochemically in purified nuclear and cytoplasmic extracts prepared from suspension and adherent cells. Jurkat cells (Fig. 6C, lanes 1 to 4) and N-Tera 2 cells (Fig. 6C, lanes 5 to 8) both contained nuclear and cytoplasmic Dlc-1, indicating that subcellular Dlc-1 localization was unchanged in both suspension and adherent cells. Hybridization of the same Western blot with anti-α-tubulin antibody was used as a control to validate the fractionation procedure.

Cell stimulation by TNF-α leads to a rapid proteolysis of IκBα and induces high levels of NF-κB activity. To investigate whether TNF-α stimulation affected the subcellular distribution of Dlc-1, both cell populations were either treated with 10 ng of TNF-α per ml for 15 min (Fig. 6C, lanes 3, 4, 7, and 8) or left untreated (Fig. 6C, lanes 1, 2, 5, and 6) prior to cell fractionation. The subcellular localization of Dlc-1 remained unchanged after TNF-α stimulation. Taken together, these data indicate that Dlc-1 displays cytoplasmic and nuclear localization.

Dlc-1 and IκBα colocalize in the cytoplasm. In higher organisms, cytoplasmic dynein is associated with cytoskeleton-mediated motility events such as slow axonal transport (21). In addition, the newly characterized human Dlc-1 isoform has been reported to be a cytoplasmic protein (19). For these reasons, we expected to find Dlc-1 mainly associated with cytosolic components. However, as shown by biochemical fractionation and by indirect immunofluorescence, transfected Myc-tagged Dlc-1 was localized either in the cytoplasm, in the nucleus, or simultaneously in both compartments of the same cell (see Fig. 7 to 9). The Myc antibody was unable to recognize endogenous c-Myc, since untransfected cells remained unstained (data not shown). The same result was obtained when the anti-Dlc-1 antibody was used on the same slide, indicating that the Myc tag did not affect localization; also, the same localization of Dlc-1 was observed in untransfected cells, thus ruling out the possibility that overexpression of Dlc-1 could saturate cellular transporters (data not shown).

To determine the site(s) of subcellular colocalization of Dlc-1 and IκBα, double-label immunofluorescence confocal microscopy was performed with COS-1 cells transfected with a Myc-tagged Dlc-1 expression plasmid and an NF-κB RelA(p65) plasmid to induce endogenous expression of IκBα (14, 39, 63). As shown in Fig. 7, induced, endogenous IκBα (fluorescein isothiocyanate [FITC] fluorescence) localized predominantly to the cytoplasm while Dlc-1 (rhodamine fluorescence) localized to both the nucleus and cytoplasm (Fig. 7A and C). Merged dual-channel images revealed that the two proteins colocalized to large areas of the cytoplasm, as shown by the

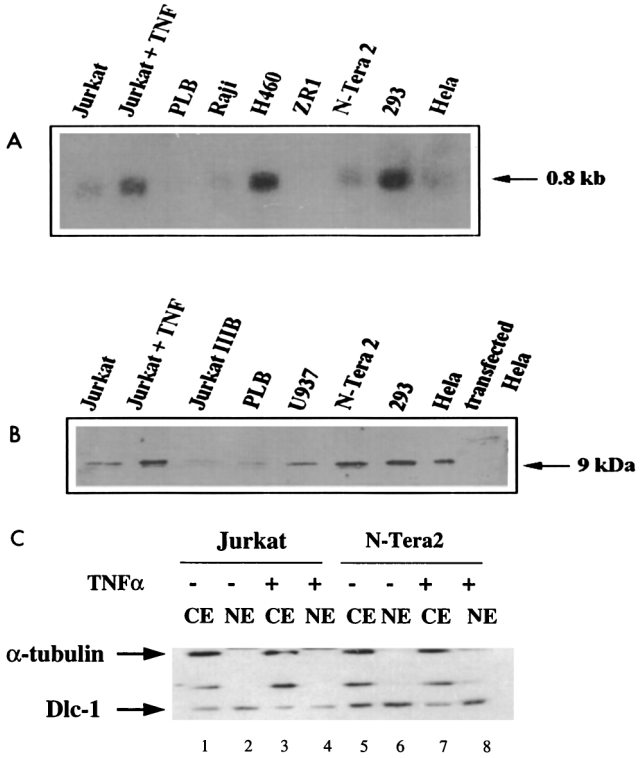

FIG. 6. Dlc-1 is a ubiquitously expressed, cytoplasmic and nuclear protein. (A) Total RNA (20 μg) from hematopoietic cells (Jurkat, PLB, Raji, H460, and ZR1), from embryonal carcinoma cells (N-Tera-2), or from adherent fibroblastic cells (293 and HeLa) were analyzed for expression of hDlc-1 RNA by Northern blotting with a ^{32}P-labeled Dlc-1 probe. Jurkat cells were treated with TNF-α at 10 ng/ml for 4 h prior to RNA isolation. Longer exposure of the autoradiograph revealed that all cells contained hDlc-1-specific RNA. (B) Total protein extracts (40 μg) prepared from hematopoietic cells (Jurkat, Jurkat-IIIB PLB, and U937), from embryonal carcinoma cells (N-Tera-2), and from fibroblastic cells (293 and HeLa) were analyzed for hDlc-1 protein expression by immunoblot analysis with a Dlc-1-specific antibody. (C) Jurkat cells and N-Tera 2 cells treated with TNF-α (10 ng/ml) for 15 min or untreated were biochemically fractionated into nuclear and cytoplasmic components. CE, cytoplasmic extract; NE, nuclear extract. α-Tubulin signal is shown as a control to validate the fractionation procedure. The middle band is an α-tubulin degradation product.

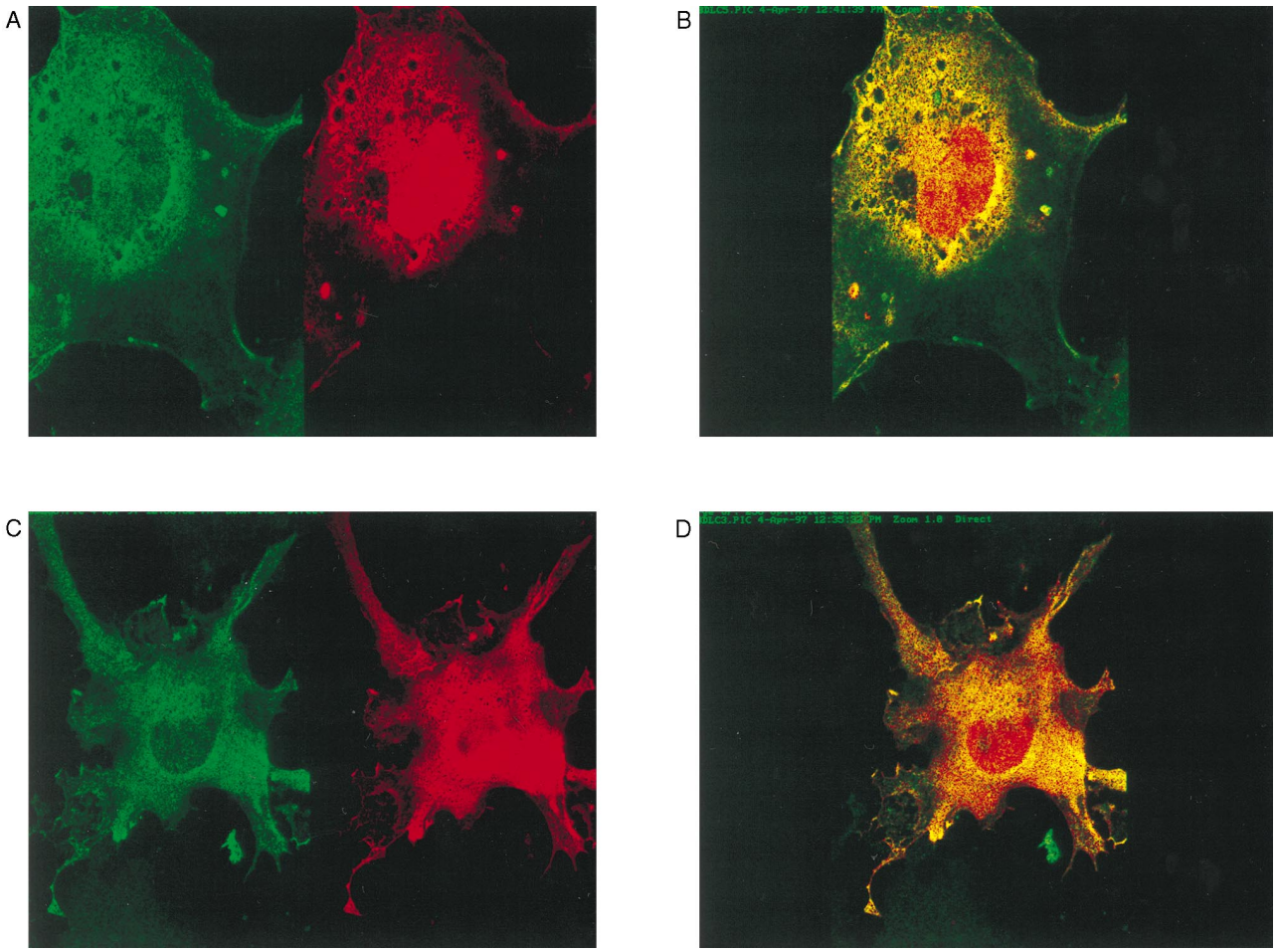

FIG. 7. Cytoplasmic colocalization of IκBα and Dlc-1. Cells were transfected with 125 ng of NF-κB RelA and Myc-tagged Dlc-1 expressed from the pSVK3 expression plasmid for 48 h before fixation. After coupling to FITC- and rhodamine-conjugated antibodies, slides were analyzed by confocal microscopy. Scale: 1 cm = 100 μm. (A and C) The FITC-conjugated antibody detected p65-induced IκBα (green), and the rhodamine-coupled antibody detected Dlc-1 (red). (B and D) Colocalization of the two proteins is detected by the yellow fluorescence generated by merging the color images.

yellow fluorescence in the merged color images (Fig. 7B and D). To further confirm the colocalization of IκBα and Dlc-1, we also performed vertical cross-sectional analysis of Myc-Dlc-1- and NF-κB RelA-transfected cells (Fig. 8). Again, IκBα localized mainly to the cytoplasm while hDlc-1 stained both the nucleus and cytoplasm of the cell (Fig. 8A); the merged-color image revealed a striking immunolocalization of IκBα and Dlc-1 exclusively to the cytoplasm, with a distinct red nucleus (Fig. 8B). Two vertical cross sections were also generated by rotating the merged dual-channel images and analyzing a slice through the nucleus (Fig. 8C) and a slice through the cytoplasm (Fig. 8D). In Fig. 8C, the large red nucleus containing hDlc-1 and areas of IκBα and Dlc-1 cytoplasmic colocalization revealed in the vertical axis by yellow staining can be seen. Similarly, the vertical cross section of the cytoplasm demonstrated yellow regions of IκBα and Dlc-1 colocalization (Fig. 8D).

hDlc-1 and IκBα colocalize with the microtubule network. Many studies have shown that dyneins are associated with microtubules; Dlc-1 has likewise been shown to colocalize with microtubules (19, 36). Confocal microscopy analysis performed on COS-1 cells transfected with Myc–Dlc-1 demonstrated that Dlc-1 associated with the microtubule network (Fig. 9A and C) but also clearly demonstrated an association with the perinuclear microtubule organizing center (MTOC) (Fig. 9B and D). The results obtained by confocal microscopy analysis prompted us to investigate whether IκBα also associated with the microtubule network. As shown in Fig. 10A, IκBα and α-tubulin both localized to the cytoplasm of COS-1 cells transfected with Myc–Dlc-1 and RelA(p65) expression plasmids. Strikingly, the merging of the dual-channel images colocalized IκBα and α-tubulin in the cytoplasm to a subset of microtubules; furthermore, the association of IκBα and α-tubulin was focused to a perinuclear region that includes the MTOC, the region from which the microtubules radiate (Fig. 10B). Two vertical cross sections of IκBα and α-tubulin immunolocalization were also obtained (Fig. 11) by rotating the merged dual-channel images and analyzing two cytoplasmic slices. The positions of the vertical cross sections can be seen in Fig. 11A as the lines of reduced fluorescence. Both the upper (Fig. 11B) and lower (Fig. 11C) cross sections revealed extensive colocalization of IκBα and α-tubulin. Together with the confocal data demonstrating the colocalization of hDlc-1 and α-tubulin, as well as genetic, biochemical, and immunolocalization data demonstrating hDlc-1 and IκBα association, these results identify Dlc-1 as a protein that acts as a bridge between the NF-κB–IκBα transcription factors and the cytoskeletal microtubule network.

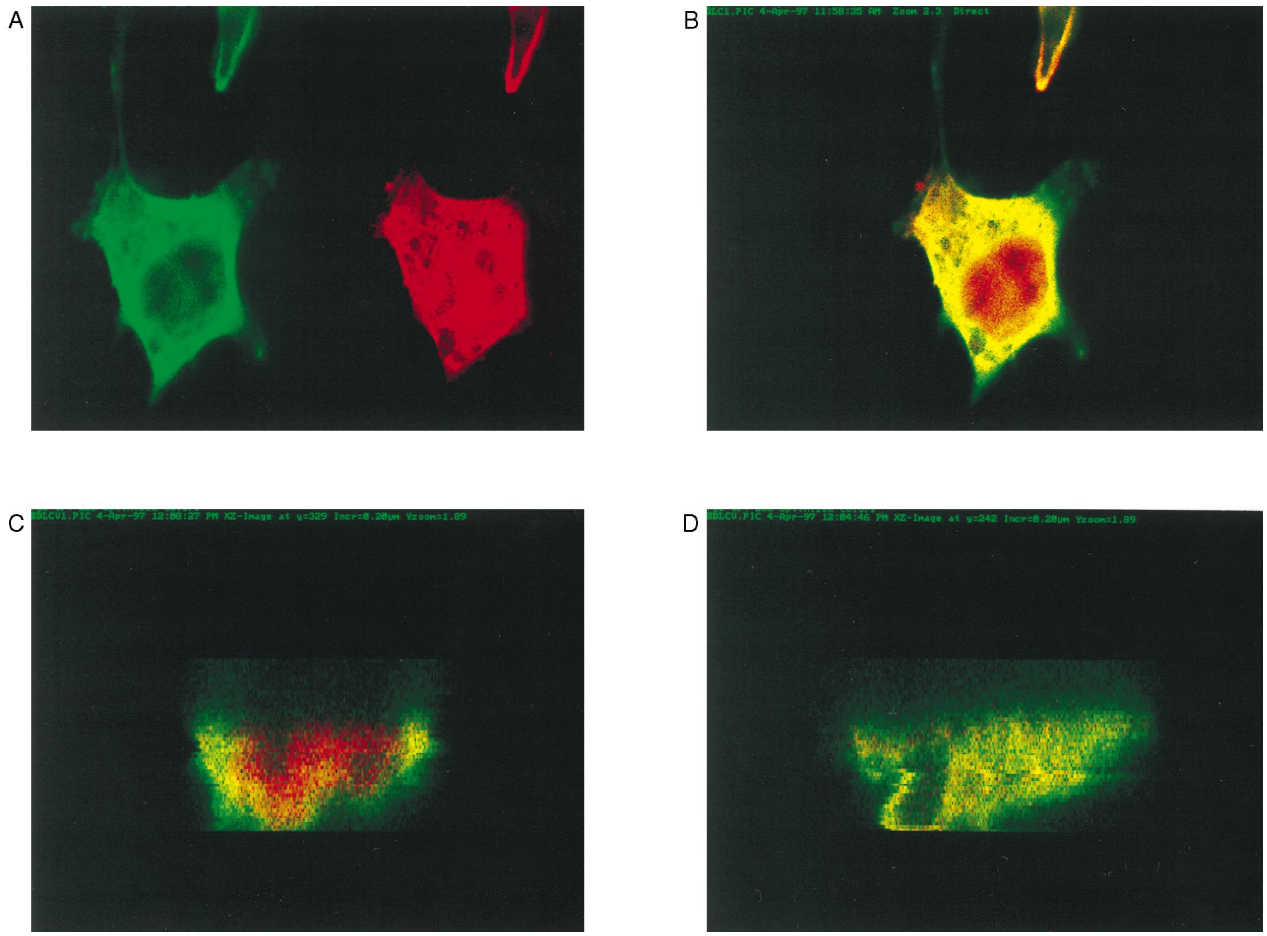

FIG. 8. Vertical and horizontal cross sections of IκBα and hDlc-1. COS-1 cells were transfected, fixed, and stained as described in the legend to Fig. 7. (A) The FITC-conjugated antibody detected p65-induced IκBα (green), and the rhodamine-coupled antibody detected Dlc-1 (red). (B) Colocalization of the two proteins is detected by the yellow fluorescence generated by merging the color images. (C) The merged color image was rotated, and a vertical cross-sectional analysis through the nucleus was performed. (D) The merged color image was rotated, and a vertical cross-sectional analysis through the cytoplasm was performed.

DISCUSSION

In this report, we demonstrate that the IκBα protein associates physically with Dlc-1, a cytoskeleton-associated dynein light-chain protein of 9 kDa. This interaction was originally detected in a yeast two-hybrid genetic screen, with the N terminus of IκBα (aa 1 to 55) as bait and an LMP-1-transformed B-lymphocyte library; in this assay, we identified several independent clones of hDlc-1, including both hDlc-1a and a splicing variant, hDlc-1b. Interestingly, in a previous HeLa cell library screen, we had also picked up a Dlc-1 clone (18a). This interaction did not compromise the ability of IκBα to associate with NF-κB RelA(p65). Surprisingly, although IκBα ankyrin repeats were expected to mediate contacts with integral membrane proteins and with the cytoskeleton, we found that only the signal response domain was required for cytoskeleton association. We also demonstrated that Dlc-1 displayed both cytoplasmic and nuclear subcellular distribution; both IκBα and hDlc-1 proteins clearly colocalize within the cytoplasm as determined by dual-fluorescence confocal microscopy. Furthermore, both Dlc-1 and IκBα interacted with the microtubule network, particularly with the MTOC.

Dyneins are large multisubunit ATPases divided into inner and outer arms, each composed of multiple heavy, intermediate, light intermediate, and light chains (69). These proteins are molecular motors that provide the driving force for microtubule-based transport within cells (69). They also contact the actin cytoskeleton through the dynactin complex (28). The dynein complex is thought to be responsible for retrograde transport as well as centripetal transport of endosomes, lysosomes, and elements of the Golgi apparatus (69). Evidence of a role for cytoplasmic dyneins in mitosis also exists (51, 68). However, little is known about the function of individual dynein chains and, least of all, about the 9-kDa outer-arm dynein light chain.

Recently, the first cytoplasmic dynein light chain of *Drosophila* (DDLC1) and its human counterpart were cloned (19, 36). The Dlc-1 protein reported here is homologous to these and includes the variant Dlc-1b form which was also picked up in the two-hybrid screen. In *Drosophila*, P-element-induced partial loss-of-function mutations caused pleiotropic morphogenetic defects in bristle and wing development, as well as in oogenesis, resulting in female sterility. Interestingly, the majority of total loss-of-function mutant animals degenerated during embryogenesis, and dying cells showed morphological changes characteristic of apoptosis (19). Therefore, DDLC1 appears to play a role in the inhibition of apoptosis during *Drosophila* development. It will be interesting to determine whether human Dlc-1 displays a biological function in mam-

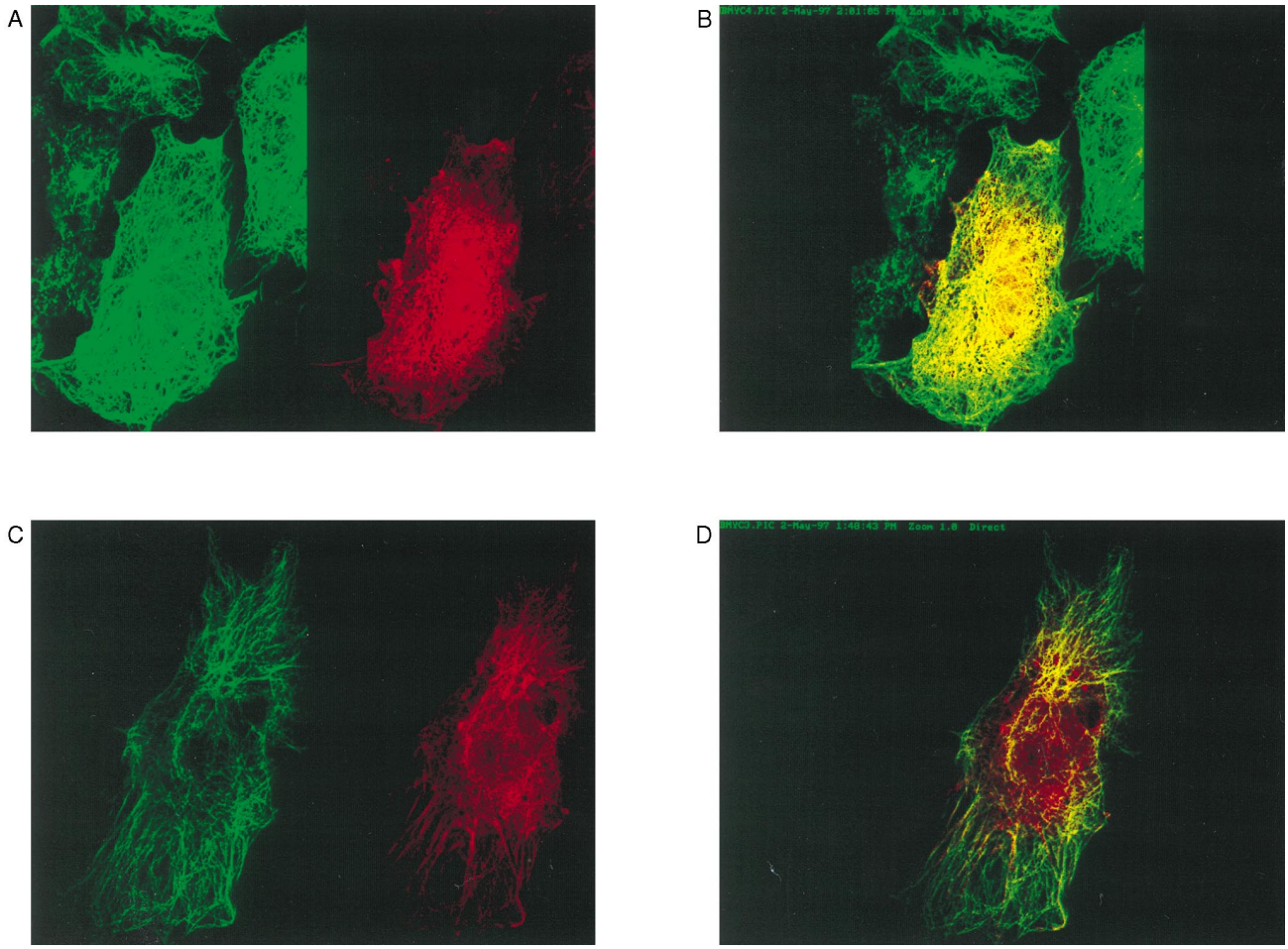

FIG. 9. hDlc-1 and α-tubulin colocalize to the microtubule cytoskeleton. COS-1 cells were transfected with 125 ng of the Myc-tagged Dlc-1 expression plasmid for 48 h prior to fixation. (A and C) FITC-labeled α-tubulin is shown on the left (green), and rhodamine-labeled hDlc-1 is shown on the right. (B and D) Colocalization of the two proteins is detected by the yellow fluorescence generated by merging the color images. The MTOC is prominently labeled by both conjugated antibodies (yellow).

malian cells similar to that revealed by DDLC1 mutants, particularly given recent evidence that NF-κB can play a protective role in TNF-α-induced apoptosis (38, 62, 64).

The results reported here raise a number of appealing hypotheses. First, we demonstrate that Dlc-1 does not interfere with IκBα binding to the RelA(p65) subunit of NF-κB. RelA(p65) knockout mice suffer from a severe liver degeneration due to massive apoptosis (11), suggesting that p65 limits pro-

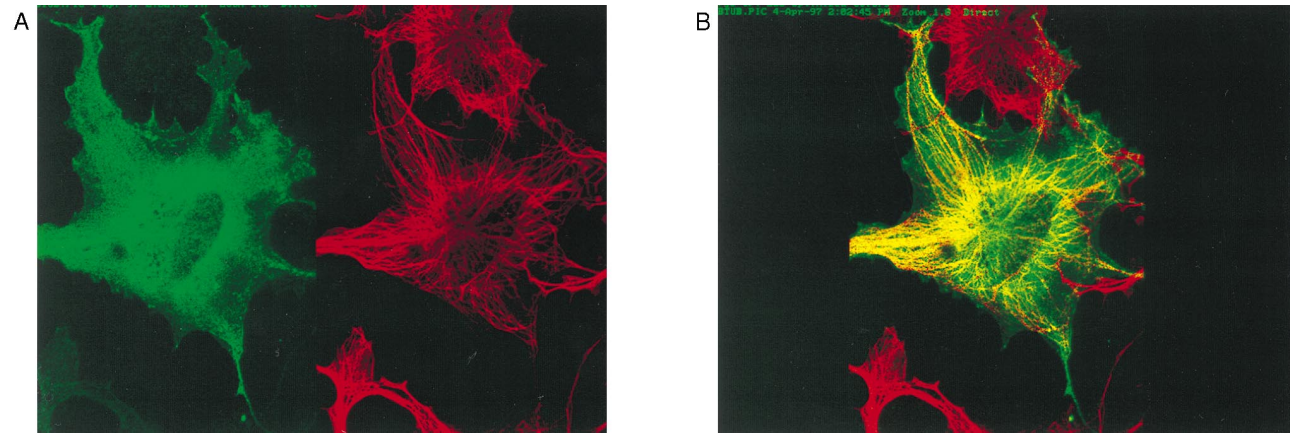

FIG. 10. Association of IκBα with the MTOC. COS-1 cells were transfected with 125 ng of NF-κB RelA expression plasmid to induce endogenous IκBα expression. At 48 h after transfection, cells were fixed and stained. After coupling to FITC- and rhodamine-conjugated antibodies, slides were analyzed by confocal microscopy. Scale: 1 cm = 100 μm. (A) IκBα is detected by the FITC-conjugated antibodies (green), and α-tubulin is detected by the rhodamine-conjugated antibody (red). (B) Colocalization of IκBα and α-tubulin is visualized in yellow by merging the color images. IκBα localizes to a subset of microtubules in the region of the MTOC.

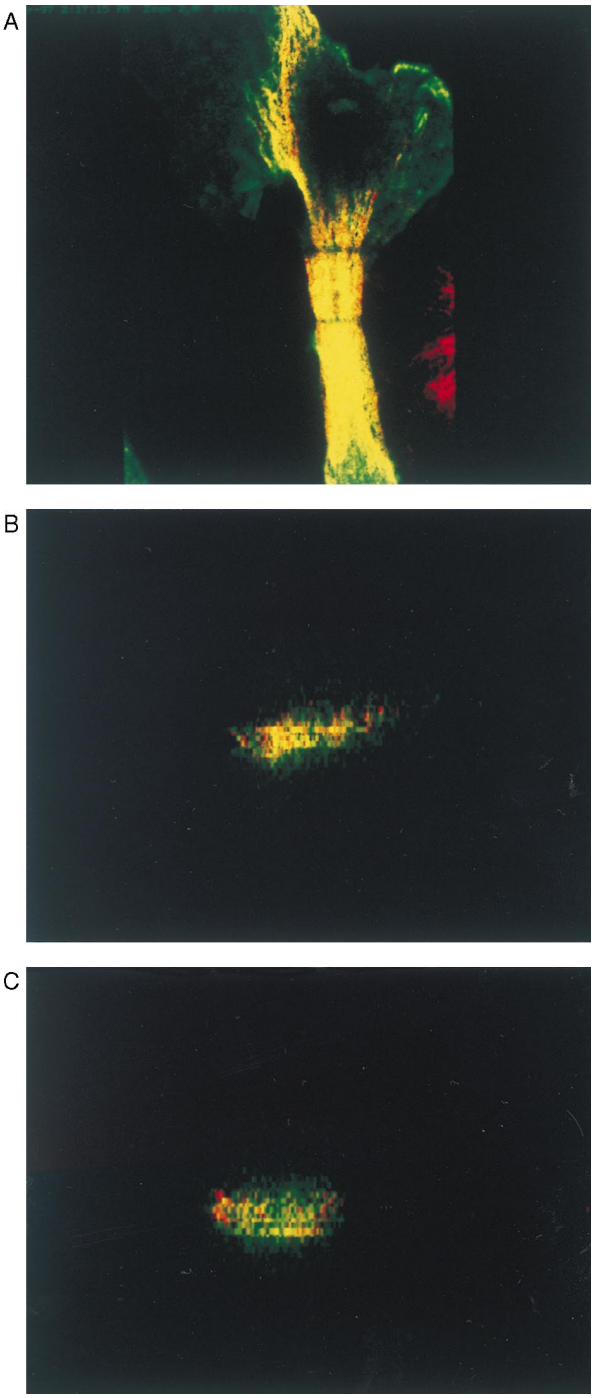

FIG. 11. Vertical and horizontal cross sections of IκBα and α-tubulin. COS-1 cells were transfected, fixed, and stained as described in the legend to Fig. 7. (A) FITC-conjugated antibody detected p65-induced IκBα (green), the rhodamine-coupled antibody detected α-tubulin (red), and colocalization of the two proteins was detected by the yellow fluorescence generated by merging the color images. (B and C) The merged color image was rotated, and a vertical cross-sectional analysis through the cytoplasm was performed. The positions of the vertical cross sections can be seen in panel A as the lines of reduced fluorescence. Both the upper (B) and lower (C) cross sections revealed extensive colocalization of IκBα and α-tubulin.

grammed cell death in liver cells. In contrast, forced c-Rel expression in chicken bone marrow cells induces apoptosis (1). If the DDLC1 inhibitory role in apoptosis appears to be conserved in mammals, it will be of great interest to examine whether Dlc-1 could modulate IκBα–c-Rel interaction, perhaps altering the ratio of c-Rel-containing to p65-containing complexes. It is also possible that Dlc-1 may strengthen the IκBα–c-Rel interaction in order to prevent the apoptosis program, while as shown here, the IκBα-p65 association would remain unaffected.

Second, DDLC1 is cytoskeleton associated and seems to be exclusively cytoplasmic. In contrast, it is shown here that human Dlc-1 has both cytosolic and nuclear distribution, and this distinct subcellular distribution may reflect functional differences. Of note, newly synthesized IκBα accumulates in the nucleus of cells following brief exposure to TNF-α (4) and could be actively exported to the cytosol via a putative nuclear export signal located at its carboxy-terminal end (5, 24). Whether Dlc-1 affects intracellular trafficking of NF-κB–IκB complexes is being investigated.

Third, our results highlight the possibility that IκBα additionally contributes to the cytoplasmic retention of NF-κB through an interaction with cytoskeletal components. This interaction may allow the activity state of NF-κB to be modulated by the cytoarchitecture and may provide a mechanism for gene regulation in response to cytoskeletal changes. This hypothesis is supported by recent studies demonstrating that a variety of agents and conditions that depolymerize microtubules but not the actin cytoskeleton rapidly activate NF-κB and induce NF-κB-dependent gene expression (58). This activation is accompanied by concomitant IκBα proteolysis. Of note, ubiquitin and ubiquitin-activating enzymes are also localized to microtubules (49, 67). During the preparation of this article, Régnier et al. identified conserved helix-loop-helix ubiquitous kinase (CHUK) as an IκB kinase capable of phosphorylating Ser-32 and Ser-36, modifications that are required for targeted degradation of IκBα via the ubiquitin-proteasome pathway (54). It will obviously be of great importance to determine the relationship between CHUK, microtubule depolymerization, and NF-κB/IκB activation. In addition, rac1 has been reported to be part of a redox-dependent signal transduction pathway leading to NF-κB activation (17). The results presented here provide a molecular link between cytoskeletal dynamics and NF-κB-dependent gene regulation by highlighting an intriguing association between the IκBα protein and the human homolog of a member of the dynein family of motor proteins.

ACKNOWLEDGMENTS

This work was supported by grants from the National Cancer Institute, the Medical Research Council of Canada and the Canadian Foundation for AIDS Research to J.H. P.C. was the recipient of fellowships from the Association pour le Recherche sur le Cancer, from the Lady Tata Foundation, and from the Fondation pour la Recherche en Santé du Québec. H.K. is a recipient of a studentship from FCAR.

We thank Normand Pepin and Sonia Cisternas for excellent technical assistance, Diane Gingras (University of Montreal) for help with confocal microscopy, Jean Coll (Institut Pasteur de Lille, Lille, France) for critical reading of the manuscript, and Vincent Laudet (Institut Pasteur de Lille, Lille, France) for assistance in sequence database searches.

REFERENCES

1. **Abbadie, C., N. Kabrun, F. Bouali, J. Smardova, D. Stehelin, B. Vandenbunder, and P. J. Enrietto.** 1993. High levels of c-Rel expression are associated with programmed cell death in the developing avian embryo and in bone marrow cells *in vitro*. Cell **75:**899–912.
2. **Alkalay, I., A. Yaron, A. Hatzubai, S. Jung, A. Avraham, O. Gerlitz, I. Pashut-Lavon, and Y. Ben-Neriah.** 1995. In vivo stimulation of IκB phosphorylation is not sufficient to activate NF-κB. Mol. Cell. Biol. **15:**1294–1301.
3. **Alkalay, I., A. Yaron, A. Hatzubai, A. Orian, A. Ciechanover, and Y. Ben-Neriah.** 1995. Stimulation-dependent IκBα phosphorylation marks the

NF-κB inhibitor for degradation *via* the ubiquitin-proteasome pathway. Proc. Natl. Acad. Sci. USA **92:**10599–10603.
4. **Arenzana-Seisdedos, F., J. Thompson, M. S. Rodriguez, F. Bachelerie, D. Thomas, and R. T. Hay.** 1995. Inducible nuclear expression of newly synthesized IκBα negatively regulates DNA-binding and transcriptional activities of NF-κB. Mol. Cell. Biol. **15:**2689–2696.
5. **Arenzana-Seisdedos, F., P. Turpin, M. Rodriguez, D. Thomas, R. T. Hay, J.-L. Virelizier, and C. Dargemont.** 1997. Nuclear localization of IκBα promotes active transport of NF-κB from the nucleus to the cytoplasm. J. Cell Sci. **110:**369–378.
6. **Baeuerle, P. A., and D. Baltimore.** 1988. Activation of DNA-binding activity in an apparently cytoplasmic precursor of the NF-κB transcription factor. Cell **53:**211–217.
7. **Baeuerle, P. A., and D. Baltimore.** 1988. IκB: a specific inhibitor of the NF-κB transcription factor. Science **242:**540–546.
8. **Beauparlant, P., I. Kwan, R. Bitar, P. Chou, A. E. Koromilas, N. Sonenberg, and J. Hiscott.** 1994. Disruption of IκBα regulation by antisense RNA expression leads to malignant transformation. Oncogene **9:**3189–3197.
9. **Beauparlant, P., R. Lin, and J. Hiscott.** 1996. The role of the C-terminal domain of IκBα in protein degradation and stability. J. Biol. Chem. **271:** 10690–10696.
10. **Beg, A. A., S. M. Ruben, R. I. Scheinman, S. Haskill, C. A. Rosen, and A. S. Baldwin, Jr.** 1992. IκB interacts with the nuclear localization sequence of the subunits of NF-κB: a mechanism for cytoplasmic retention. Genes Dev. **6:**1899–1913.
11. **Beg, A. A., W. C. Sha, R. T. Bronson, S. Ghosh, and D. Baltimore.** 1995. Embryonic lethality and liver degeneration in mice lacking the RelA component of NF-κB. Nature **376:**167–170.
12. **Brockman, J. A., D. C. Scherer, T. A. McKinsey, S. M. Hall, X. Qi, W. Y. Lee, and D. W. Ballard.** 1995. Coupling of a signal response domain in IκBα to multiple pathways for NF-κB activation. Mol. Cell. Biol. **15:**2809–2818.
13. **Brown, K., S. Gerstberger, L. Carlson, G. Franzoso, and U. Siebenlist.** 1995. Control of IκB-α proteolysis by site-specific, signal-induced phosphorylation. Science **267:**1485–1488.
14. **Brown, K., S. Park, T. Kanno, G. Franzoso, and U. Siebenlist.** 1993. Mutual regulation of the transcriptional activator NF-κB and its inhibitor, IκB-α. Proc. Natl. Acad. Sci. USA **90:**2532–2536.
15. **Chen, Z., J. Hagler, V. J. Palombella, F. Melandri, D. Scherer, D. Ballard, and T. Maniatis.** 1995. Signal-induced site-specific phosphorylation targets IκBα to the ubiquitin-proteasome pathway. Genes Dev. **9:**1586–1597.
16. **Chen, Z. J., L. Parent, and T. Maniatis.** 1996. Site-specific phosphorylation of IκBα by a novel ubiquitination-dependent protein kinase activity. Cell **84:**853–862.
17. **Chu, Z.-L., T. A. McKinsey, L. Liu, X. Qi, and D. W. Ballard.** 1996. Basal phosphorylation of the PEST domain in IκBβ regulates its functional interaction with the c-*rel* proto-oncogene product. Mol. Cell. Biol. **16:**5974–5984.
18. **Craig, S. W., and R. P. Johnson.** 1996. Assembly of focal adhesions: progress, paradigms, and portents. Curr. Opin. Cell Biol. **8:**74–85.
18a. **Crépieux, P.** Unpublished data.
19. **Dick, T., K. Ray, H. K. Salz, and W. Chia.** 1996. Cytoplasmic dynein (*ddlc1*) mutations cause morphogenetic defects and apoptotic cell death in *Drosophila melanogaster*. Mol. Cell. Biol. **16:**1966–1977.
20. **DiDonato, J. A., F. Mercurio, and M. Karin.** 1995. Phosphorylation of IκBα precedes but is not sufficient for its dissociation from NF-κB. Mol. Cell. Biol. **15:**1302–1311.
21. **Dillman, J. F., III, L. P. Dabney, and K. K. Pfister.** 1996. Cytoplasmic dynein is associated with slow axonal transport. Proc. Natl. Acad. Sci. USA **93:**141–144.
22. **Evan, G. I., G. K. Lewis, G. Ramsay, and J. M. Bishop.** 1985. Isolation of monoclonal antibodies specific for human c-*myc* proto-oncogene product. Mol. Cell. Biol. **5:**3610–3616.
23. **Finco, T. S., A. A. Beg, and A. S. Baldwin, Jr.** 1994. Inducible phosphorylation of IκBα is not sufficient for its dissociation from NF-κB and is inhibited by protease inhibitors. Proc. Natl. Acad. Sci. USA **91:**11884–11888.
24. **Fritz, C. C., and M. R. Green.** 1996. HIV Rev uses a conserved cellular protein export pathway for the nucleocytoplasmic transport of viral RNAs. Curr. Biol. **6:**848–854.
25. **Frost, J. A., S. Xu, M. R. Hutchison, S. Marcus, and M. H. Cobb.** 1996. Actions of Rho family small G proteins and p21-activated protein kinases on mitogen-activated protein kinase family members. Mol. Cell. Biol. **16:**3707–3713.
26. **Fuerst, T. R., E. G. Niles, F. W. Studier, and B. Moss.** 1986. Eukaryotic transient-expression system based on recombinant vaccinia virus that synthesizes T7 RNA polymerase. Proc. Natl. Acad. Sci. USA **83:**8122–8126.
27. **Gilmore, T., and P. Morin.** 1993. The IκB proteins: members of a multifunctional family. Trends Genet. **9:**427–433.
28. **Glotzer, M., and A. A. Hyman.** 1995. The importance of being polar. Curr. Biol. **5:**1102–1105.
29. **Hatada, E. N., M. Naumann, and C. Scheidereit.** 1993. Common structural constituents confer IκB activity to NF-κB p105 and IκB/MAD-3. EMBO J. **12:**2781–2788.
30. **Hollenberg, S. M., R. Sternglanz, P. F. Cheng, and H. Weintraub.** 1995. Identification of a new family of tissue-specific basic helix-loop-helix proteins with a two-hybrid system. Mol. Cell. Biol. **15:**3813–3822.
31. **Imbert, V., R. A. Rupec, A. Livolsi, H. L. Pahl, E. B.-M. Traenckner, C. Mueller-Dieckmann, D. Farahifar, B. Rossi, P. Auberger, P. A. Baeuerle, and J.-F. Peyron.** 1996. Tyrosine phosphorylation of IκB-α activates NF-κB without proteolytic degradation of IκB-α. Cell **86:**787–798.
32. **Ingber, D. E.** 1993. The riddle of morphogenesis: a question of solution chemistry or molecular cell engineering? Cell **75:**1249–1252.
33. **Inoue, J. I., L. D. Kerr, D. Rashid, N. Davis, and H. R. Bose, Jr.** 1992. Direct association of pp40/IκBβ with rel/NF-κB transcription factors: role of ankyrin repeats in the inhibition of DNA binding activity. Proc. Natl. Acad. Sci. USA **89:**4333–4337.
34. **Jaffray, E., K. M. Wood, and R. T. Hay.** 1995. Domain organization of IκBα and sites of interaction with NF-κB p65. Mol. Cell. Biol. **15:**2166–2172.
35. **Katagari, K., T. Katagari, K. Kajiyama, T. Yamamoto, and T. Yoshida.** 1993. Tyrosine-phosphorylation of tubulin during monocytic differentiation of HL-60 cells. J. Immunol. **150:**585–593.
36. **King, S. M., E. Barbares, J. F. Dillman, R. S. Patel-King, J. H. Carson, and K. K. Pfister.** 1996. Brain cytoplasmic and flagellar outer arm dyneins share a highly conserved Mr8,000 light chain. J. Biol. Chem. **271:**19358–19366.
37. **King, S. M., and R. S. Patel-King.** 1995. The M_r = 8,000 and 11,000 outer arm dynein light chains from *Chlamydomonas* flagella have cytoplasmic homologues. J. Biol. Chem. **270:**11445–11452.
38. **Kontgen, F., R. J. Grumont, A. Strasser, D. Metcalf, R. Li, D. Tarlington, and S. Gerondakis.** 1995. Mice lacking the c-*rel* proto-oncogene exhibit defects in lymphocyte proliferation, humoral immunity and interleukin-2 expression. Genes Dev. **9:**1965–1977.
39. **Le Bail, O., R. Schmidt-Ullrich, and A. Israël.** 1993. Promoter analysis of the gene encoding the IκBα/MAD-3 inhibitor of NF-κB: positive regulation by members of the rel/NF-κB family. EMBO J. **12:**5043–5049.
40. **Lee, F. S., J. Hagler, Z. J. Chen, and T. Maniatis.** 1997. Activation of the IκBα kinase complex by MEKK1, a kinase of the JNK pathway. Cell **88:** 213–222.
41. **Lee, J. S., D. von der Ahe, B. Kiefer, and Y. Nagamine.** 1993. Cytoskeletal reorganization and TPA differently modify AP-1 to induce the urokinase-type plasminogen activator gene in LLC-PK_1 cells. Nucleic Acids Res. **21:** 3365–3372.
42. **Lin, R., P. Beauparlant, C. Makris, S. Meloche, and J. Hiscott.** 1996. Phosphorylation of IκBα in the C-terminal PEST domain by casein kinase II affects intrinsic protein stability. Mol. Cell. Biol. **16:**1401–1409.
43. **Lin, Y.-C., K. Brown, and U. Siebenlist.** 1995. Activation of NF-κB requires proteolysis of the inhibitor IκB-α: signal-induced phosphorylation of IκB-α alone does not release active NF-κB. Proc. Natl. Acad. Sci. USA **92:**552–556.
44. **Lux, S. E., K. M. John, and V. Bennett.** 1990. Analysis of cDNA for human erythrocyte ankyrin indicates a repeated structure with homology to tissue-differentiation and cell-cycle control proteins. Nature **344:**36–42.
45. **Manie, S., A. Schmid-Alliana, J. Kubar, B. Ferrua, and B. Rossi.** 1993. Disruption of microtubule network in human monocytes induces expression of interleukin-1 but not that of interleukin-6 or tumor necrosis factor-α. J. Biol. Chem. **268:**13675–13681.
46. **Miyamoto, S., M. Maki, M. J. Schmitt, M. Hatanaka, and I. M. Verma.** 1994. Tumor necrosis factor α-induced phosphorylation of IκBα is a signal for its degradation but not dissociation from NF-κB. Proc. Natl. Acad. Sci. USA **91:**12740–12744.
47. **Morin, P., G. S. Subramanian, and T. D. Gilmore.** 1993. GAL4-IκBα and GAL4-IκBγ activate transcription by different mechanisms. Nucleic Acids Res. **21:**2157–2163.
48. **Morin, P. J., and T. D. Gilmore.** 1992. The c-terminus of the NF-κB p50 precursor and an IκB isoform contain transcription activation domains. Nucleic Acids Res. **20:**2453–2455.
49. **Murti, K. G., H. T. Smith, and V. A. Fried.** 1988. Ubiquitin is a component of the microtubule network. Proc. Natl. Acad. Sci. USA **85:**3019–3023.
50. **Negrutskii, B. S., and M. P. Deutscher.** 1992. A sequestered pool of aminoacyl-tRNA in mammalian cells. Proc. Natl. Acad. Sci. USA **89:**3601–3604.
51. **Niclas, J., V. J. Allan, and R. D. Vale.** 1996. Cell cycle regulation of dynein association with membranes modulates microtubule-based organelle transport. J. Cell Biol. **133:**585–593.
52. **Nobes, C. D., P. Hawkins, L. Stephens, and A. Hall.** 1995. Activation of the small GTP-binding proteins rho and rac by growth factor receptors. J. Cell Sci. **108:**225–232.
53. **Pepin, N., A. Roulston, J. Lacoste, R. Lin, and J. Hiscott.** 1994. Subcellular redistribution of HTLV-1-Tax protein by NF-κB/Rel transcription factors. Virology **204:**706–716.
54. **Régnier, C., H. Y. Song, X. Gao, D. V. Goeddel, Z. Cao, and M. Rothe.** 1997. Identification and characterization of an IκB kinase. Cell **90:**373–383.
55. **Reszka, A. A., R. Seger, C. D. Diltz, E. G. Krebs, and E. H. Fisher.** 1995. Association of mitogen-activated protein kinase with the microtubule cytoskeleton. Proc. Natl. Acad. Sci. USA **92:**8881–8885.
56. **Richard, S., D. Yu, K. J. Blumer, D. Hausladen, M. W. Olszowy, P. A. Connelly, and A. S. Shaw.** 1995. Association of p62, a multifunctional SH2- and SH3-domain-binding protein, with src family tyrosine kinases, Grb2, and phospholipase Cγ-1. Mol. Cell. Biol. **15:**186–197.

57. **Rodriguez, M. S., J. Wright, J. Thompson, D. Thomas, F. Baleux, J. L. Virelizier, R. T. Hay, and F. Arenzana-Seisdedos.** 1996. Identification of lysine residues for signal-induced ubiquitination and degradation of IκBα *in vivo*. Oncogene **12:**2425–2435.
58. **Rosette, C., and M. Karin.** 1995. Cytoskeletal control of gene expression: depolymerization of microtubules activates NF-κB. J. Cell. Biochem. **128:** 1111–1119.
59. **Scherer, D. C., J. A. Brockman, Z. Chen, T. Maniatis, and D. W. Ballard.** 1995. Signal-induced degradation of IκBα requires site-specific ubiquitination. Proc. Natl. Acad. Sci. USA **92:**11259–11263.
60. **Schiestl, R. H., and R. D. Gietz.** 1989. High efficiency transformation of intact yeast cells using single stranded nucleic acids as a carrier. Curr. Genet. **16:**339–346.
61. **Shaw, A. S., K. E. Amrein, C. Hammond, D. F. Stern, B. M. Sefton, and J. K. Rose.** 1989. The *lck* tyrosine protein kinase interacts with the cytoplasmic tail of the CD4 glycoprotein through its unique amino-terminal domain. Cell **59:**627–636.
62. **Sulciner, D. J., K. Irani, Z.-X. Yu, V. J. Ferrans, P. Goldschmidt-Clermont, and T. Finkel.** 1996. rac1 regulates a cytokine-stimulated, redox-dependent pathway necessary for NF-κB activation. Mol. Cell. Biol. **16:**7115–7121.
63. **Sun, S.-C., P. A. Ganchi, D. W. Ballard, and W. C. Greene.** 1993. NF-κB controls expression of inhibitor IκBα: evidence for an inducible autoregulatory pathway. Science **259:**1912–1915.
64. **Suyang, H., R. Phillips, I. Douglas, and S. Ghosh.** 1996. Role of unphosphorylated, newly synthesized IκBβ in persistent activation of NF-κB. Mol. Cell. Biol. **16:**5444–5449.
65. **Traenckner, E. B.-M., S. Wilk, and P. A. Baeuerle.** 1994. A proteasome inhibitor prevents activation of NF-κB and stabilizes a newly phosphorylated form of IκB-α that is still bound to NF-κB. EMBO J. **13:**5433–5441.
66. **Traenckner, E. B. M., H. L. Pahl, T. Henkel, K. N. Schmidt, S. Wilk, and P. A. Baeuerle.** 1995. Phosphorylation of human IκBα on serines 32 and 36 controls IκBα proteolysis and NF-κB activation in response to diverse stimuli. EMBO J. **14:**2876–2883.
67. **Trausch, J. S., S. J. Grenfell, P. M. Handley-Gearhart, A. Ciechanover, and A. L. Schwartz.** 1993. Immunofluorescent localization of the ubiquitin-activating enzyme, E1, to the nucleus and cytoskeleton. Am. J. Physiol. **264:** C93–C102.
68. **Vaisberg, E. A., M. P. Koonce, and J. R. McIntosh.** 1993. Cytoplasmic dynein plays a role in mammalian mitotic spindle formation. J. Cell Biol. **123:**849–858.
69. **Vallee, R.** 1993. Molecular analysis of the microtubule motor dynein. Proc. Natl. Acad. Sci. USA **90:**8769–8772.
70. **Verma, I. M., J. K. Stevenson, E. M. Schwarz, D. V. Antwerp, and S. Miyamoto.** 1995. Rel/NF-κB/IκB family: intimate tales of association and dissociation. Genes Dev. **9:**2723–2735.